



HAL
open science

Functional characterization of a vacuolar invertase from *Solanum lycopersicum*: Post-translational regulation by N-glycosylation and a proteinaceous inhibitor

Alexandra Tauzin, Gerlind Sulzenbacher, Mickael Lafond, Véronique Desseaux, Ida Barbara Reca, Josette Perrier, Daniela Bellincampi, Patrick Fourquet, Christian Levêque, Thierry Giardina

► To cite this version:

Alexandra Tauzin, Gerlind Sulzenbacher, Mickael Lafond, Véronique Desseaux, Ida Barbara Reca, et al.. Functional characterization of a vacuolar invertase from *Solanum lycopersicum*: Post-translational regulation by N-glycosylation and a proteinaceous inhibitor. *Biochimie*, 2014, 101, pp.39-49. 10.1016/j.biochi.2013.12.013 . hal-01793351

HAL Id: hal-01793351

<https://hal.science/hal-01793351>

Submitted on 12 Apr 2023

HAL is a multi-disciplinary open access archive for the deposit and dissemination of scientific research documents, whether they are published or not. The documents may come from teaching and research institutions in France or abroad, or from public or private research centers.

L'archive ouverte pluridisciplinaire **HAL**, est destinée au dépôt et à la diffusion de documents scientifiques de niveau recherche, publiés ou non, émanant des établissements d'enseignement et de recherche français ou étrangers, des laboratoires publics ou privés.

Copyright

Provided for non-commercial research and education use.
Not for reproduction, distribution or commercial use.



This article appeared in a journal published by Elsevier. The attached copy is furnished to the author for internal non-commercial research and education use, including for instruction at the authors institution and sharing with colleagues.

Other uses, including reproduction and distribution, or selling or licensing copies, or posting to personal, institutional or third party websites are prohibited.

In most cases authors are permitted to post their version of the article (e.g. in Word or Tex form) to their personal website or institutional repository. Authors requiring further information regarding Elsevier's archiving and manuscript policies are encouraged to visit:

<http://www.elsevier.com/authorsrights>



Contents lists available at ScienceDirect

Biochimie

journal homepage: www.elsevier.com/locate/biochi

Research paper

Functional characterization of a vacuolar invertase from *Solanum lycopersicum*: Post-translational regulation by N-glycosylation and a proteinaceous inhibitor



Alexandra S. Tauzin^{a,1}, Gerlind Sulzenbacher^b, Mickael Lafond^a, Véronique Desseaux^a,
Ida Barbara Reça^{c,2}, Josette Perrier^a, Daniela Bellincampi^c, Patrick Fourquet^d,
Christian Lévêque^e, Thierry Giardina^{a,*}

^a Aix Marseille Université, Centrale Marseille, CNRS, iSm2 UMR 7313, 13397 Marseille, France

^b Aix Marseille Université, CNRS, AFMB UMR 7257, 13288 Marseille, France

^c Dipartimento di Biologia e Biotecnologie "Charles Darwin", "Sapienza" Università di Roma, Roma, Italy

^d Centre d'Immunologie de Marseille Luminy, Service Protéomique, 13288 Marseille, France

^e Aix Marseille Université, CNRS, Plateformes de Recherche en Neurosciences/CAPM, UMR 7286, 13344 Marseille, France

ARTICLE INFO

Article history:

Received 26 July 2013

Accepted 13 December 2013

Available online 27 December 2013

Keywords:

Vacuolar invertase

Proteinaceous inhibitor

N-Glycosylation

Surface plasmon resonance

Solanum lycopersicum

Protein–protein interactions

ABSTRACT

Plant vacuolar invertases, which belong to family 32 of glycoside hydrolases (GH32), are key enzymes in sugar metabolism. They hydrolyse sucrose into glucose and fructose. The cDNA encoding a vacuolar invertase from *Solanum lycopersicum* (TIV-1) was cloned and heterologously expressed in *Pichia pastoris*. The functional role of four N-glycosylation sites in TIV-1 has been investigated by site-directed mutagenesis. Single mutations to Asp of residues Asn52, Asn119 and Asn184, as well as the triple mutant (Asn52, Asn119 and Asn184), lead to enzymes with reduced specific invertase activity and thermostability. Expression of the N516D mutant, as well as of the quadruple mutant (N52D, N119D, N184D and N516D) could not be detected, indicating that these mutations dramatically affected the folding of the protein. Our data indicate that N-glycosylation is important for TIV-1 activity and that glycosylation of N516 is crucial for recombinant enzyme stability. Using a functional genomics approach a new vacuolar invertase inhibitor of *S. lycopersicum* (SolyVIF) has been identified. *SolyVIF* cDNA was cloned and heterologously expressed in *Escherichia coli*. Specific interactions between SolyVIF and TIV-1 were investigated by an enzymatic approach and surface plasmon resonance (SPR). Finally, qRT-PCR analysis of *TIV-1* and *SolyVIF* transcript levels showed a specific tissue and developmental expression. *TIV-1* was mainly expressed in flowers and both genes were expressed in senescent leaves.

© 2013 Elsevier Masson SAS. All rights reserved.

1. Introduction

In higher plants β -D-fructofuranosyl-(2 \rightarrow 1)- α -D-glucopyranoside (sucrose) is the major transport form of carbohydrates and it is

both a source of carbon skeletons and energy for plant organs unable to perform photosynthesis. Sucrose is produced in the source tissues and transported *via* the phloem to the different sink tissues where it is hydrolysed by invertases (β -fructofuranosidases, **EC 3.2.1.26**) or by sucrose synthases (**EC 2.4.1.13**) into glucose and fructose, or UDP-glucose and fructose, respectively, which subsequently are used in different biochemical pathways [1].

Several isoforms of invertases have been identified and different types are distinguished [2]. According to their pH optima, they are classified into two major groups, acid invertases and neutral or alkaline invertases. While neutral and alkaline invertases can be localized in the cytosol, mitochondria or in plastids, acid invertases are linked to the cell wall (cell wall invertases) or found in vacuoles (vacuolar invertases). Acid invertases belong to glycoside hydrolase family GH32 (<http://www.cazy.org/>) [3], which comprises acid invertases from plants, fungal and bacterial endo- and exo-inulinases,

Abbreviations: CIF, cell wall inhibitor of β -fructosidase; DNS, dinitrosalicylic acid; Endo H, endoglycosidase H; GH, glycoside hydrolase; INH, invertase inhibitor; PME1, inhibitor of pectin methylesterase; PME1-RP, pectin methylesterase inhibitor related protein; QM, quadruple mutant; SolyVIF, *Solanum lycopersicum* vacuolar invertase inhibitor; SPR, surface plasmon resonance; TIV-1, *Solanum lycopersicum* vacuolar invertase; TM, triple mutant; VIF, vacuolar inhibitor of β -fructosidase.

* Corresponding author. Tel.: +33 4 9128 8445; fax: +33 4 9128 8440.

E-mail address: thierry.giardina@univ-amu.fr (T. Giardina).

¹ Present address: Michael Smith Laboratories and Department of Chemistry, University of British Columbia, 2185 East Mall, Vancouver, BC V6T 1Z4, Canada.

² Present address: Great Lakes Bioenergy Research Center, Michigan State University, East Lansing, USA.

levanases, plant fructan exohydrolases (FEHs) and plant fructan biosynthetic enzymes.

Invertases have multiple functions – notably they are involved in early plant development, most likely *via* control of sugar composition and metabolic fluxes [4,5]. Biochemical and physiological studies suggest that cell wall invertases play a key role in regulation of phloem unloading and sucrose partitioning [2,6], cell differentiation and plant development [7,8], as well as in regulation of the response to various biotic and abiotic stresses [9–11]. The proposed functions of vacuolar invertases include regulation of turgor and cell enlargement [12,13], control of the sugar composition in fruits and storage organs [14–16], and involvement in the response to wounding [11], cold [17], drought [18], hypoxia [19], and gravitropism [20]. In contrast to acid invertases, cytoplasmic invertases have been less investigated at the functional level, but evidence is growing that they play a role in plant growth and development and that they might be involved in oxidative stress response [21,22].

Regulation of acid invertases occurs at the transcriptional and translational levels following various stimuli such as hexose concentration or environmental changes [23,24]. N-Glycosylation, where a glycan chain is attached in the endoplasmic reticulum to an Asn residue of the acceptor proteins, is one of these important co- and post-translational modifications. N-Glycosylation of yeast invertases has been broadly studied and is known to have a crucial role in protein stability [25–28]. In plants, acid invertases are known to be glycosylated proteins and it has been shown that N-glycosylation of these enzymes is important for stability, transport and secretion [29,30]. Some differences in N-glycan chain composition have been noticed between cell wall and vacuolar invertases [31].

Invertase activity can also be regulated by endogenous proteinaceous inhibitors (INHs). INHs were first described in the 1960s in *Solanum tuberosum* [32] and later purified by Pressey [33]. More recently INHs were studied in other organisms such as *Nicotiana tabacum* [34], *Arabidopsis thaliana* [35], *Coffea canephora* [36], and *Solanum lycopersicum* [37]. INHs belong to the pectin methylesterase inhibitor related protein (PMEI-RP) family (Pfam 04043), together with pectin methylesterase inhibitors (PMEIs) [38]. INHs are named according to their subcellular localization: Cell-wall Inhibitor of β -Fructosidases (CIF) and Vacuolar Inhibitor of β -Fructosidases (VIF). INHs are named C/VIF when the subcellular localization is not clear or when they inhibit both vacuolar and cell wall invertases. Although the physiological function of INHs has not yet been established, it has recently been reported that the increase of CWI activity by silencing CIF delayed leaf senescence and increased seed weight and fruit hexose levels in tomato [16]. It has been shown that the resistance to cold-induced sweetening in potato depends on the post-translational regulation of the vacuolar invertase by its inhibitor and that both proteins are localized in the same compartment [39–41]. The decrease of invertase inhibitor activity in source leaves *via* down-regulation of INH expression is also part of the plant defence response [42].

Until now, the most comprehensive study on how vacuolar invertase could be regulated at a post-translational level by proteinaceous inhibitor was performed on the partners from potato [39–41,43]. In tomato most studies carried out so far focused on the cell wall partners [16,37]. In the present study we aimed at a better understanding of two independent mechanisms involved in the post-translational regulation of vacuolar invertase from *S. lycopersicum* (hereafter called TIV-1): N-glycosylation and inhibition by a proteinaceous inhibitor. Previously TIV-1 has been shown to be N-glycosylated and identified as a potent human allergen (named Lyc e 2 in that study [44]). In this paper, the role of

N-glycosylation in protein folding was studied by expressing diverse variants lacking one or more N-glycosylations and by investigating the impact of single or multiple mutations on enzyme activity and stability. Using a functional genomics approach, a new VIF of *S. lycopersicum* (hereafter called SolyVIF) was identified, cloned and characterized. Specific interactions between SolyVIF and TIV-1 were investigated by an enzymatic approach and surface plasmon resonance (SPR). And finally, the expression of TIV-1 and SolyVIF mRNA was explored in different plant tissues.

2. Material and methods

2.1. Cloning, expression and purification of vacuolar invertase (TIV-1) and vacuolar inhibitor (SolyVIF) from *S. lycopersicum*

For TIV-1, mRNA from red tomato fruit was amplified by RT-PCR, using specific primers (Supplementary Table S1), for 30 PCR cycles at an annealing temperature of 42 °C. The PCR product was directly cloned in the pPICZ α A-derived *Pichia pastoris* expression plasmid and sequenced by Beckman Coulter Genomics (Takeley, UK). Mutations were introduced into the pPICZ α A::TIV-1 plasmid using the QuickChange XL Site-directed Mutagenesis kit (Stratagene Europe, Amsterdam Zuidoost, The Netherlands). Two overlapping complementary oligonucleotides containing the corresponding nucleotide changes were designed for each mutation (Table S1). Mutations were confirmed by DNA sequencing. Transformation of cells and selection of positive clones were performed as described previously [45]. Large-scale expression was carried out as described previously [46]. For purification of recombinant TIV-1 and its variants, the culture supernatant was subjected to ammonium sulphate precipitation up to 80%, dialysed and loaded onto a size exclusion column (Sephacryl S-200). The fractions containing invertase activity were pooled.

For SolyVIF, the clone (SGN-U332870 which was superseded in 2009 by SGN-U567308) containing the complete open reading frame of SolyVIF was obtained from the Boyce Thompson Institute for Plant Research (New York, USA). The PCR products amplified with the In-Fusion primers (Table S1) were combined with the expression vector pOPINF following the manufacturer's instructions (In-Fusion™, BD-Clontech). The recombinant vectors were checked by double stranded DNA sequencing (Beckman Coulter Genomics, Takeley, UK). In-Fusion™ system led to the production of SolyVIF with a (His)₆ tag at the N-terminus. The *Escherichia coli* Rosetta *gami* strain, which possesses a pRARE plasmid for supplying tRNAs for rare codons and mutations in trxB/gor facilitating cytoplasmic disulfide bond formation, was transformed with the recombinant vector. Transformants were grown at 37 °C in selective LB media. Gene expression was induced with 1 mM isopropyl- α -D-thiogalactopyranoside (Sigma) when the optical density reached 0.6. After for 4 h at 37 °C, the cells were collected by centrifugation at 4000 g for 15 min. Cells were resuspended in 20 mM sodium phosphate, 0.5 M NaCl and 20 mM imidazole buffer pH 7.4 and lysed by addition of lysozyme (200 μ g mL⁻¹ resuspension buffer) and Benzonase (25 U mL⁻¹ resuspension buffer). After 30 min of incubation at room temperature, cell debris was pelleted by centrifugation (12,000 g, 30 min, 4 °C). Solubilization of inclusion bodies was carried out by incubating the pellet with 5 mL resuspension buffer containing 6 M urea in ice for 1 h. The mix was centrifuged (12,000 g, 30 min, 4 °C) and the supernatant was recovered. Purification was performed using immobilized metal ion affinity chromatography (IMAC) (GE Healthcare) according to the manufacturer's instructions. The fractions containing the eluted protein were pooled and dialysed against 40 mM Na-acetate buffer pH 4.6.

2.2. Vacuolar invertase activity and determination of kinetic parameters

TIV-1 activity was measured at pH 4.5 and 50 °C for 10 min using the dinitrosalicylic acid (DNS) assay [47] with some modifications as described by Reca et al. [37]. The optimal pH was determined on sucrose in McIlvaine's buffer (0.1 M citric acid, 0.2 M sodium phosphate) in a pH range of 3.5–7.0. Activity was expressed in micromoles of released reducing sugar/min/mg protein.

Kinetic parameters were determined at optimal conditions of pH and temperature in Na-acetate buffer pH 4.5 at 50 °C, by incubating 6 pM of TIV-1 with sucrose concentrations ranging from 10 to 150 mM.

Effect of SolyVIF on the invertase activity was determined on sucrose at pH 4.5. The inhibition constant (K_i) was determined at 50 °C for 10 min after pre-incubating TIV-1 with various concentrations of inhibitor (7–28 nM) at different substrate concentrations (10–150 mM).

2.3. SDS-polyacrylamide gel electrophoresis (SDS-PAGE), N-deglycosylation and periodic acid Schiff staining

Protein denaturing SDS-PAGE was performed on 10–15% polyacrylamide gels. Gels were stained with Coomassie Brilliant Blue R-250 [48]. Protein concentrations were determined by the method of Bradford [49].

Purified TIV-1 (10 µg) was N-deglycosylated using 1000 units of Endo H (New England's Biolabs) and the reaction was performed following the supplier recommendations.

For determination of glycosylation levels, SDS-polyacrylamide gels were stained with periodic acid-Schiff stain using the SIGMA glycoprotein Detection Kit[®] according to the manufacturer's protocol.

2.4. N-Terminal sequencing

After SDS-PAGE, the protein transfer was performed on a polyvinylidene difluoride membrane in transfer buffer (50 mM Tris/HCl and 50 mM boric acid, pH 8.3) on constant amperage (250 mA) for 4 h at 4 °C. First of all, in order to be activated, the membrane was immersed in three bashes successively: 10 s in methanol, 1–2 min in water, then 10 min in transfer buffer. Quality of transfer was confirmed by Ponceau red staining (0.2% Ponceau and 3% trichloroacetic acid). Band of interest protein was cut and automated repetitive Edman degradation was performed on a model 494 Procise[™] (Applied Biosystems) at Institut Pasteur (Paris).

2.5. Mass spectrometry analyses

Mass analyses were performed on a MALDI-TOF-TOF Bruker Ultraflex III spectrometer (Bruker Daltonics) controlled by the Flexcontrol 3.0 package (Build 51). This instrument was used at a maximum accelerating potential of 25 kV and was operated in linear mode at the m/z range from 20,000 to 100,000. Five external standards (Protein Calibration Standard II, Bruker Daltonics) were used to calibrate each spectrum to a mass accuracy within 100 ppm. One µL of sample was mixed with 1 µL of sinapinic acid matrix in an acetonitrile/0.1% trifluoroacetic acid mixture (1:2) and 1 µL was spotted on the target, dried and analysed. Peak picking was performed with the Flexanalysis 3.0 software (Bruker Daltonics).

2.6. Surface plasmon resonance (SPR)

SPR experiments were performed at 25 °C on a Biacore 3000 (GE Healthcare) instrument. About 150–250 response units (RU) of TIV-

1 were coupled on CM3 sensor chips at pH 4.5 using the amine coupling kit (GE Healthcare). A control flow cell was activated and deactivated in the same way, but without protein injection, to yield a blank surface. SPR measurements were performed by injecting various dilutions of SolyVIF in running buffer (20 mM Na-acetate, 130 mM NaCl, 2.5 mM spermine and 0.05% Tween 20, pH 4.5) at 30 µL min⁻¹. For each sample injection, interactions were monitored simultaneously in the different flow cells. Regeneration was performed after each injection with 200 mM Tris-HCl pH 8.0. Analysis of biosensor data was performed using the Biaevaluation 3.1 control software. The stoichiometry of the SolyVIF/TIV-1 interaction was calculated using the formula: (analyte maximum response/immobilization response) × (ligand MW/analyte MW).

2.7. RT-PCR and qRT-PCR

Total RNA was isolated from induced *P. pastoris* cultures following the supplier recommendations (Invitrogen[™]). cDNAs were generated from diverse *P. pastoris* clones through reverse-transcription (RT-PCR) using SuperScript[®]VIL0[™] cDNA Synthesis Kit following the supplier recommendations (Invitrogen[™]). cDNA were amplified with DNA polymerase (Platinum[®] Taq DNA Polymerase, Invitrogen[™]) according to the manufacturer's instructions. RT-PCR was performed with the following oligonucleotide primers: *VINVfor* and *VINVrev*, *AOX2for* and *AOX2rev* (Table S1) using an iCycler (Biorad).

Quantitative RT-PCR was performed as previously described [37] and using the following oligonucleotide primers: *SolyVIFfor* and *SolyVIFrev*, *TIV-1for* and *TIV-1rev*, *ACT4for* and *ACT4rev* (Table S1). The expression level of the gene of interest was normalized to the expression of the actin gene (*ACT4*) using a modified version of the Pfaffl method [50].

2.8. Bioinformatic analyses

Nucleotide and amino acid sequences of SolyVIF (SGN-U567308) were identified within the Solanaceae Cornell University Data Bank (www.sgn.cornell.edu). The theoretical isoelectric point and molecular mass were predicted using Compute pI/Mw (http://web.expasy.org/compute_pi/). The signal peptide and location of the putative signal peptide cleavage site were predicted using the SignalP 3.0 Server (<http://www.cbs.dtu.dk/services/SignalP/>). Putative N- and O-glycosylation sites were predicted using the NetNGlyc 1.0 Server (<http://www.cbs.dtu.dk/services/NetNGlyc/>) and the DictyOGlyc 1.1 Server (<http://www.cbs.dtu.dk/services/DictyOGlyc/>), respectively. All alignments were performed with ClustalW2 (<http://www.ebi.ac.uk/Tools/msa/clustalw2/>) [51]. The secondary structure elements were added with ESPript [52]. The kinetic parameters were estimated using non-linear regression analysis with the GraphPad Prism software (GraphPad Prism version 3.00 for Windows 95, GraphPad Software, San Diego, CA, USA, www.graphpad.com). The three-dimensional model of TIV-1 was generated with the Swiss-Model Server (<http://swissmodel.expasy.org>) using the *Pachysandra terminalis* 6-SST/6-SFT (PDB-ID 3UGF) (65% sequence identity with TIV-1) as template. Figures were prepared with Pymol [53].

3. Results and discussion

3.1. Vacuolar invertase expression and characterization

For many years, plant invertases have received much attention mainly due to their central role in metabolic functions, stress signalling and biotechnological utilization. Plant vacuolar invertases are synthesized as pre-pro-proteins with a leader sequence

containing a signal peptide and an N-terminal extension [54]. The pro-region contains vacuolar sorting determinants essential for vacuolar trafficking [55]. The vacuolar invertase from *S. lycopersicum* (TIV-1) without the N-terminal extension, corresponding to the mature form found in tomato fruit as described by Reca et al. (2008) [37], has been expressed and characterized.

The cDNA encoding TIV-1 used in this study was cloned from red MoneyMaker tomato mRNA and the sequence was in agreement with the sequence of *TIV-1* mRNA (NCBI accession number M81081), except for a difference in position 951 corresponding to a silent mutation (ATT changed in ATC, both codons encoding Ile residue). The open reading frame of 1632 nucleotides encodes a protein of 544 amino acids with a calculated molecular mass of 60,142 Da. Based on sequence alignment, TIV-1 belongs to glycoside hydrolase family GH32 (P29000 in the Uniprot database, www.uniprot.org) according to the CAZY classification [3].

In order to perform biochemical and molecular studies, TIV-1 mature protein was heterologously expressed in *P. pastoris* using a pPICZ α A expression vector. Recombinant protein was secreted in the supernatant medium after induction with methanol. TIV-1 was purified to homogeneity, using size exclusion chromatography on a Sephacryl S200 gel (Fig. S1). After purification, a major band with

an apparent molecular mass of 79 kDa was observed on SDS-PAGE (Fig. 1A, lane 2 and 3). The N-terminal sequence EAEAYAXSNA (with X as indefinable amino acid residue, but probably Trp) was in agreement with the sequence expected for the recombinant protein, EAEA corresponding to the α -factor signal peptide C-terminal end of the pPICZ α A vector, followed by YAXSNA corresponding to the mature TIV-1 N-terminal (Fig. 1B). The protein identity was also confirmed by tryptic digestion followed by MS/MS analysis (data not shown). The purified enzyme showed a specific activity, K_m , k_{cat} and k_{cat}/K_m of 5.2 U mg $^{-1}$, 14 mM, 1384 s $^{-1}$ and 99 s $^{-1}$ mM $^{-1}$, respectively. Similar K_m values have been reported for vacuolar invertases purified from various plants, such as INV2 (12 mM) from *A. thaliana* [56] and INVII (10.5 mM) from maize [57], or heterologously expressed, such as HvINV1 (14 mM) from barley [58], I β fruct1 (10.7 mM) and I β fruct3 (10.1 mM) from potato [59,60], OsVIN2 (13.2 mM) from rice [61] and VI (15 mM) from wheat [62]. By contrast, the K_m value for sucrose of recombinant TIV-1 was slightly higher than that of the native enzyme purified from red fruit and the k_{cat} value was lower (6.4 mM and 7250 s $^{-1}$, respectively) [37]. It is noteworthy that Reca et al. (2008) used the glucose oxidase/peroxidase reagent to carry out the invertase activity assay [37]. Moreover, kinetic differences between native and

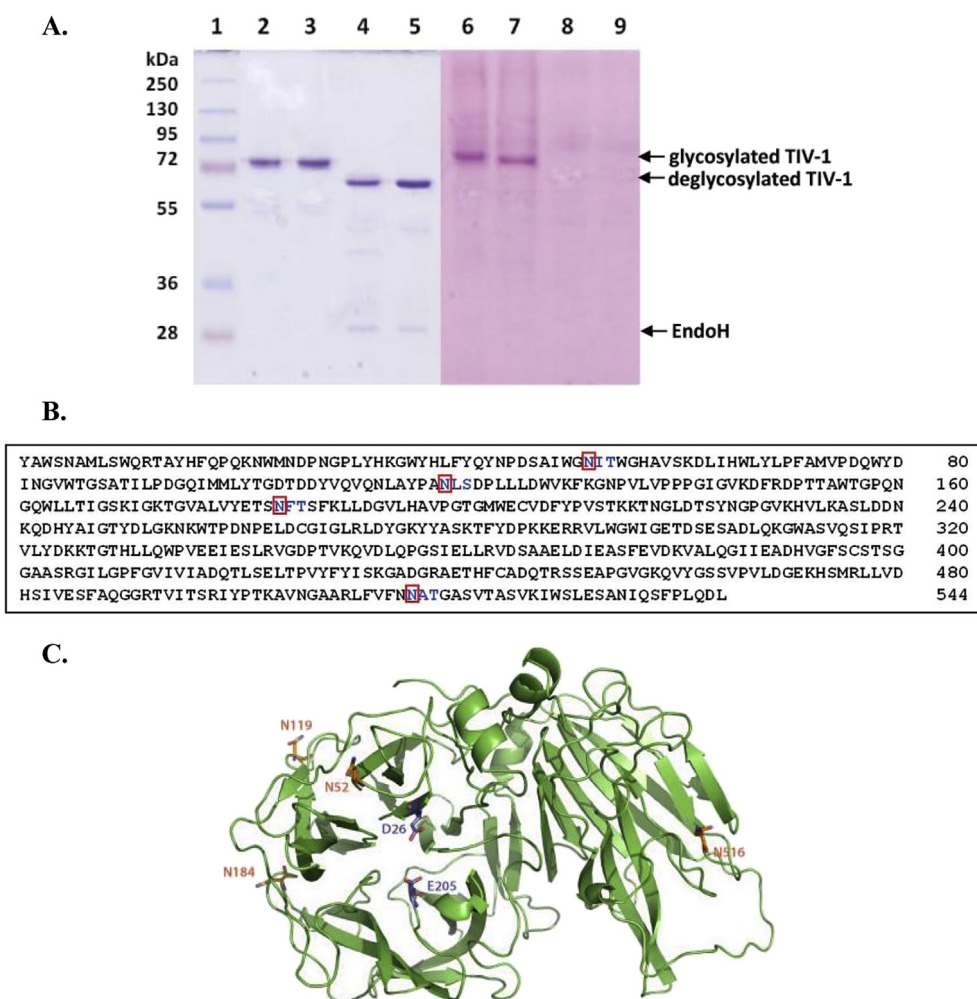


Fig. 1. **A.** Analysis of deglycosylated and not deglycosylated TIV-1 stained with Coomassie blue and Schiff's reagent. (1) molecular mass markers; (2 and 6) purified TIV-1; (3 and 7) purified TIV-1 with buffers used for N-deglycosylation; (4 and 8) purified TIV-1 heated at 100 °C and treated with Endo H; (5 and 9) purified TIV-1 not heat-denatured and treated with Endo H. **B.** Amino acid sequence of TIV-1. N-glycosylation consensus sequences are in blue with N-glycosylated residues outline in red. **C.** Molecular model of TIV-1. The model was generated by the Swiss-Model Server based on the crystal structure of the *Pachysandra terminalis* 6-SST/6-SFT (PDB-ID 3UGF). The catalytic residues (D26 and E205) are depicted in purple. N-glycosylation sites are drawn in orange.

recombinant enzymes have already been described for other systems, as for example the ones reported for sterol esterase from *Ophiostoma piceae* with comparable K_m values for native and recombinant enzyme but higher k_{cat} values for the recombinant enzyme (around 50 fold increase with the substrate *p*-nitrophenyl butyrate) [63].

3.2. TIV-1 stability and activity are regulated by N-glycosylation

The molecular mass of recombinant TIV-1 as determined by mass spectrometry (69,114 Da, data not shown) is much higher than the theoretical mass of 60,566 Da, suggesting that recombinant TIV-1 is glycosylated. Previously, native TIV-1 purified from tomato fruit has been demonstrated to be a glycoprotein [44]. Indeed, four potential N-glycosylation sites were identified in the amino acid sequence of TIV-1 at positions Asn52, Asn119, Asn184 and Asn516 (Fig. 1B), suggesting that N-glycosylation could be responsible for the observed difference in molecular mass. These sites are located far from the active site (Fig. 1C), as deduced from a homology model of TIV-1 based on the crystal structure of *P. terminalis* 6-SST/6-SFT (PDB-ID 3UGF). Two of them, Asn52 and Asn516, are in positions equivalent to two out of the four glycosylation sites observed in *P. terminalis* 6-SST/6-SFT, Asn59 and Asn516, respectively [64]. In 6-SST/6-SFT these two sites exhibit the complex glycosylation pattern typically observed in plant proteins [64]. Residues equivalent to Asn119 in TIV-1 are found to be glycosylated in the crystal structures of *A. thaliana* cell wall invertase AtcwINV1 (PDB-ID 2AC1, Asn116) [65] and *Cichorium intybus* 1-exohydrolase IIa (PDB-ID 1ST8, Asn116) [66]. None of the known crystal structures of members of GH32 display glycosylation of residues equivalent in position to TIV-1 Asn184, however this putative glycosylation site is conserved in *Aspergillus awamori* exoinulinase (PDB-ID 1Y4W) [67].

The presence of glycan chains linked to TIV-1 was revealed by periodic acid Schiff staining (Fig. 1A, lanes 6 and 7). To confirm that the difference in molecular mass was due to glycosylation, enzymatic deglycosylation was performed on heat-denatured enzyme. By gel electrophoresis, the molecular mass of TIV-1 is estimated at about 79 kDa (Fig. 1A, lane 2 and 3). After treatment with Endoglycosidase H (Endo H) to remove N-linked carbohydrate moieties, a single band located at about 70 kDa was observed on SDS-PAGE (Fig. 1A, lane 4), which corresponds to a discrepancy of about 9 kDa with respect to wild-type TIV-1 (Fig. 1A, lanes 2 and 3), close to the difference between calculated and experimental molecular masses. Furthermore, staining with Schiff's reagent after deglycosylation showed no residual staining (Fig. 1A, lane 8), which confirms that TIV-1 is only N-glycosylated. Similar results were obtained with non-denatured enzyme (Fig. 1A, lanes 5 and 9), suggesting that all N-glycosylation sites are accessible to Endo H.

To examine the role of N-linked glycosylation in TIV-1 activity, tailored alterations of TIV-1 glycosylation were performed by site-directed mutagenesis. A quadruple mutant (QM), with all four putative N-glycosylation sites mutated to Asp, was generated. In this case, QM activity and QM protein were not detected neither in the culture filtrate, where the recombinant protein is usually secreted, nor in cell extracts, indicating that glycosylation of TIV-1 plays a role in the biosynthesis and/or stability of the enzyme. To determine the contribution of each single glycosylation site, all four potentially glycosylated Asn residues were individually replaced and the four resultant mutants N52D, N119D, N184D and N516D were expressed in *P. pastoris*. As for the QM mutant, no recombinant protein was obtained for the N516D mutant (data not shown). MS/MS analyses showed that the molecular masses of the mutants N52D, N119D and N184D were slightly lower than that of TIV-1 wild-type (69,114 Da) and were equal to 67,145 Da, 67,135 Da and

67,670 Da, respectively. The calculated N-linked glycan masses on sites Asn52, Asn119 and Asn184 were 1968 Da, 1978 Da and 1443 Da, respectively. Values for Asn52 and Asn119 are in agreement with the expected masses of typical *P. pastoris* high mannose type N-glycan chains, with a mass of about 2 kDa, depending on the number of mannose residues linked at the end of the glycan chain (Man₈GlcNAc₂ or Man₉GlcNAc₂) [68]. The glycan chain linked to Asn184 is probably shorter, due to the elimination of terminal mannose residues from the high mannose core by the action of an α -1,2-mannosidase secreted by *P. pastoris* [69], and could be composed of only five or six mannose residues. A theoretical molecular mass of 3158 Da was deduced for the glycan N-linked to Asn516 (Table 1). This site, which seems to be more glycosylated (Man₁₆GlcNAc₂) than sites Asn52, Asn119 and Asn184, is close to the C-terminal of the recombinant protein and presents an Asn residue before the N-glycosylation consensus sequence (N⁵¹⁵N⁵¹⁶A⁵¹⁷T⁵¹⁸) (Fig. 1B). In 1998, Wang et al. suggested that tandem sites (NNTT) near the C-terminal of a single-chain variable fragment (Fvs) induced hyperglycosylation in recombinant protein produced by *P. pastoris* [70].

For both QM and N516D we controlled that the transformation with the pPICZ α A vector occurred on the *alcohol oxidase 1* (AOX1) locus of the yeast genome using a PCR approach on yeast genomic DNA (data not shown). Moreover, mRNA expression of mutants was confirmed by RT-PCR (Fig. S2) and likewise we verified that N516D and QM mutants were not addressed to the intracellular compartment, instead of the culture medium, by examining the absence of invertase activity in *P. pastoris* crude extract (data not shown). The absence of activity could arise from degradation of the recombinant protein or to the presence of incorrectly folded protein due to the lack of glycosylation [31]. The failure to produce both the N516D and QM active mutants points out the importance of Asn516 for correct folding and stability of recombinant TIV-1.

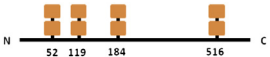
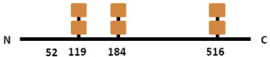
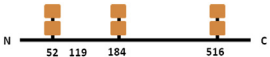
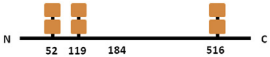
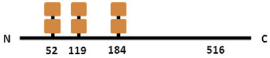
We then produced a triple mutant N52D, N119D and N184D (TM), which was expressed correctly in *P. pastoris*, indicating that glycosylation of sites Asn52, Asn119 and Asn184 was not crucial for protein folding. Next we wanted to test whether the lack of the individual glycan chains affected the activity of TIV-1. As shown in Table 1, all of the three individual mutations N52D, N119D and N184D led to a decrease of the specific activity of about 30%–60% when compared to the activity of wild-type TIV-1. Similarly, a strong decrease in overall specific activity has been reported for deglycosylated mutants of *A. thaliana* cell wall invertase (AtcwINV1) and *Beta vulgaris* fructan exohydrolase (Bv6-FEH) [65,71].

The thermal stability of each mutant as compared to the wild-type was determined at pH 4.5 (Fig. 2) and showed that N52D, N119D and TM were stable for 1 h at 40 °C, whereas N184D was stable for at least 1 h at 45 °C. After 1 h at 50 °C, TIV-1 retained its full activity, while N52D, N119D and TM retained about 50%–60% of their activity and N184D retained 70%. After 30 min at 60 °C, N52D and TM were inactive, N119D and N184D retained 15% of their activity and TIV-1 retained 30% of its activity. All recombinant proteins lost their enzymatic activity after 5 min at 65 °C. Altogether these results suggest that glycosylation of sites Asn52, Asn119 and Asn184 plays an important role in stability of recombinant TIV-1.

3.3. SolyVIF is a novel proteinaceous invertase inhibitor

After focusing on SolyCIF as potential inhibitor of TIV-1 [37], our aim was to find a putative vacuolar invertase inhibitor. Using the sequences of the well characterized vacuolar and cell-wall INHs from *N. tabacum* as template, homolog genes from tomato were searched in the Sol Genomics Networks database (http://solgenomics.net/organism/solanum_lycopersicum/genome). Based on sequence homology, a sequence encoding a putative vacuolar INH emerged,

Table 1
N-Glycosylation sites in TIV-1 and the effect on specific activity upon their site-directed removal.

Protein name	Schematic representation	Specific activity ($\mu\text{mol min}^{-1} \text{mg}^{-1}$)	MM (Da)	MM of the lacking N-linked chain (Da)
TIV-1		5.2	69,114 ^a	0 ^b
N52D		3.4	67,145 ^a	1968 ^b
N119D		3.5	67,136 ^a	1978 ^b
N184D		2.3	67,670 ^a	1443 ^b
N516D		n.d.	n.d.	3158 ^b
TM		3.3	63,724 ^b	5399 ^b
QM		n.d.	n.d.	8547 ^b

Glycosidic chains are depicted with orange squares. n.d.: not determined.

^a Determined by mass spectrometry.

^b Deduced.

identified with the number SGN-U567308, and hereafter called SolyVIF. The 528 bp *SolyVIF* gene encodes a protein of 175 amino acids and contains a signal peptide for subcellular targeting whose putative cleavage site is located between Leu16 and Asn17. Removal of the predicted N-terminal signal peptide generates mature SolyVIF of 159 amino acids with a theoretical molecular mass of 18,030 Da and a predicted isoelectric point of 5.12. SolyVIF shows highest sequence identity with vacuolar StInvlNh2A (82%) and StInvlNh2B (76%) from potato and vacuolar NtVIF (71%) from *N. tabacum*. By contrast, SolyVIF has only 43% and 45% sequence identity with cell wall NtCIF from *N. tabacum* and SolyCIF from *S. lycopersicum*, respectively. Liu et al.

proposed a phylogenetic tree of Solanaceae INHs where StInvlNh2 (corresponding to SolyVIF) belongs to the subgroup α with vacuolar StInvlNh2A, StInvlNh2B and NtInvlNh2 (NtVIF), while the subgroup β includes cell wall StInvlNh1 (SolyCIF) and NtInvlNh1 (NtCIF), suggesting a distribution according to the specificity (Fig. 2 from Ref. [40]). A specific interaction between StInvlNh2 and vacuolar invertase from potato (StvacInV1) was demonstrated by bimolecular fluorescence complementation and *in vivo* studies showed that both contributed to the cold-induced sweetening regulation [40,41]. The high sequence identity with StInvlNh2A and StInvlNh2B suggests that SolyVIF might as well have a vacuolar specificity.

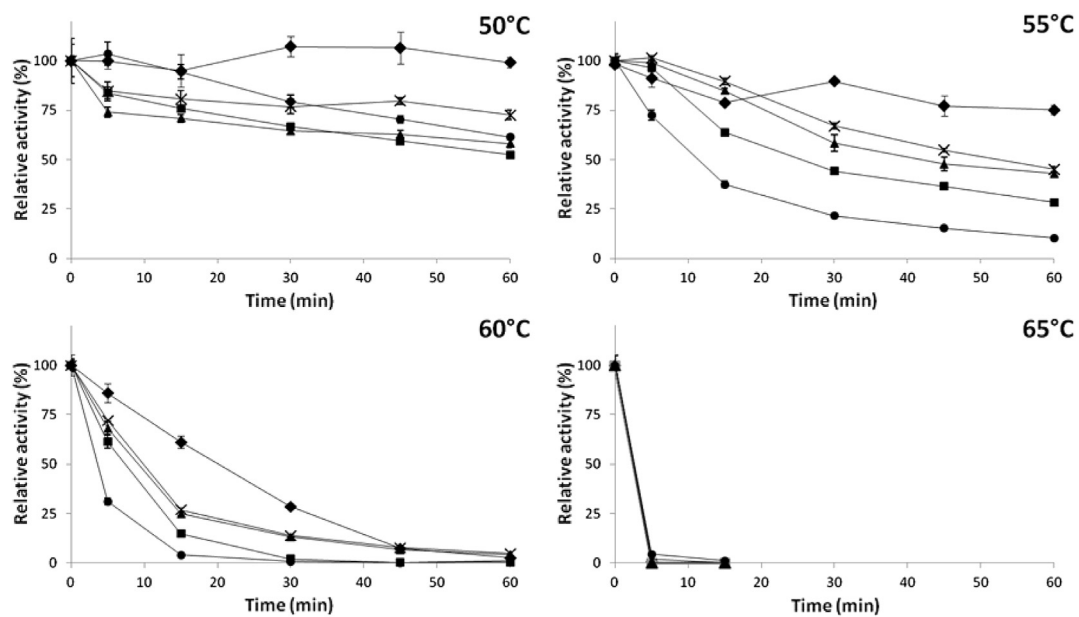


Fig. 2. Temperature stability of TIV-1 (diamond-shaped) compared to mutants N52D (square), N119D (triangle), N184D (cross) and TM (circle). Values depicted are the mean of duplicates based on at least three independent experiments.

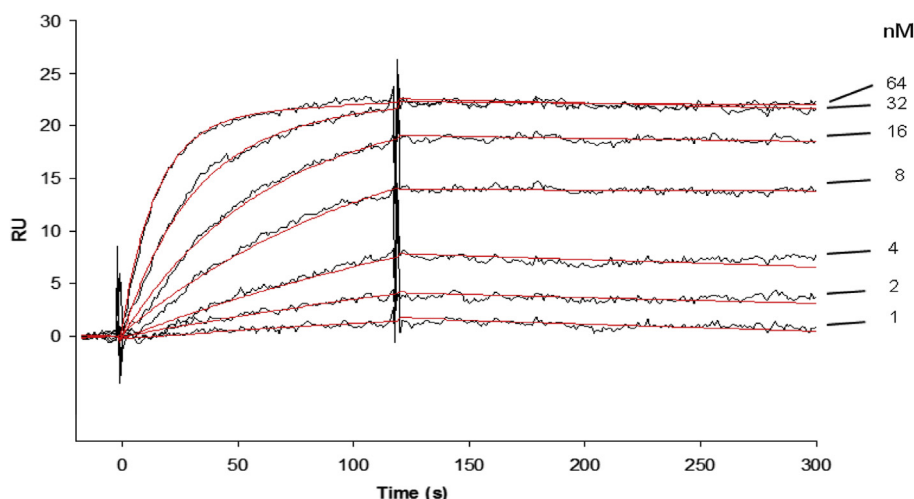


Fig. 3. SPR measurement of SolyVIF interaction with TIV-1. A set of concentrations of SolyVIF ranging from 1 to 64 nM was injected over immobilized TIV-1. The black traces represent the specific binding obtained after subtraction of a blank run and the red traces depict the global fit of the data to a simple 1:1 bimolecular Langmuir model. The data illustrated are representative of four independent experiments.

To functionally characterize the inhibitor, the *SolyVIF* cDNA was cloned into the pOPINF plasmid and expressed in *E. coli* Rosetta-gami™ (DE3) strain as a N-terminal (His)₆ tagged protein. *In vivo*, INHs are not glycosylated [72–74] and several of them have been largely expressed in *E. coli* [35,40,75,76]. It is noteworthy that heterologous expression of SolyVIF in *P. pastoris* was not successful (data not shown). After cell lysis, SolyVIF was found in inclusion bodies. Soluble protein was obtained after resolubilization with the chaotropic agent urea and purified by immobilized metal ion affinity chromatography. The expression yield was approximately 2 mg L⁻¹.

Purified SolyVIF was loaded onto SDS gel under reducing (+DTT) and non-reducing conditions (-DTT) (Fig. S3). The oxidized protein runs at an apparent molecular mass lower than the reduced protein (19 kDa vs 23 kDa), indicating that the native protein has a more compact structure compared to the denaturated protein, probably

due to the presence of the four Cys residues engaged in intramolecular disulphide bridges. Indeed, SolyVIF possesses four cysteines typically conserved in PME1-RP (Fig. S4). Indeed, crystallographic analyses of *N. tabacum* NtCIF [77], *Actinidia deliciosa* AcPME1 [78] and *A. thaliana* AtPME1-2 [38] have shown that these close homologues are composed of α -helices stabilized by two disulphide bridges [38,77,78].

3.4. TIV-1 interacts with SolyVIF

In order to assess whether SolyVIF was a genuine inhibitor of TIV-1 we analysed their potential interaction by SPR. The results of the analyses showed that there was indeed strong interaction between SolyVIF and TIV-1, with a dissociation constant value (K_D) of 0.4 ± 0.2 nM (Fig. 3). The k_{on} and k_{off} values were

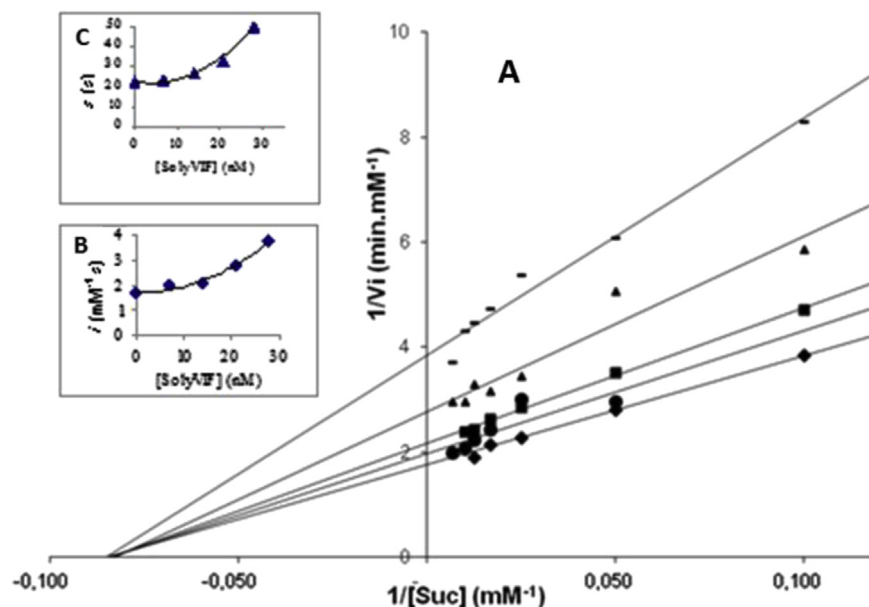


Fig. 4. Kinetic analysis of the inhibition of TIV-1 by SolyVIF using sucrose as substrate. **A.** Lineweaver–Burk plot. Hydrolysis reaction of TIV-1 on variable sucrose concentrations (10–150 mM) and at a fixed concentration of SolyVIF (0 nM, diamond-shaped; 7 nM, circle; 14 nM, square; 21 nM, triangle and 28 nM, line). TIV-1 concentration was 6.9 nM. **B, C.** Secondary plots showing the dependency of the vertical axis intercept (i) and slope (s) on the concentration of SolyVIF.

$1.2 \pm 0.5 \times 10^6 \text{ M}^{-1} \text{ s}^{-1}$ and $4.8 \pm 1.7 \times 10^{-4} \text{ s}^{-1}$, respectively. The apparent stoichiometry indicated a 1:1 interaction at equilibrium. Using isothermal titration calorimetry, a K_D in the nanomolar range and a 1:1 stoichiometry were also demonstrated for the interaction between a cell wall invertase inhibitor from *N. tabacum* (NtCIF) and a cell wall invertase from *A. thaliana* (AtcwINV1) [79].

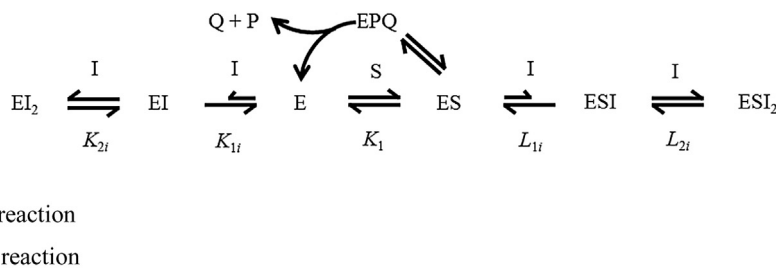
3.5. TIV-1 is inhibited by SolyVIF

The kinetic of inhibition of TIV-1 by SolyVIF was determined by enzymatic assays in solution using sucrose as substrate. Reactions were initiated by adding variable substrate concentrations of 10–150 mM in a mixture containing the enzyme (TIV-1) alone or the enzyme and the inhibitor (SolyVIF) at concentrations of 7–28 nM. Before the addition of substrate the mixture was preincubated for 10 min at 50 °C to ensure that complete equilibrium was reached between the enzyme (E), the inhibitor (I) and the enzyme–inhibitor complex (EI). Experiments confirmed that equilibrium had been reached because all of the Lineweaver–Burk plots obtained with different sucrose concentrations and fixed SolyVIF concentrations were linear (Fig. 4A). The intercept of these plots cuts the horizontal axis and accounts for non-competitive inhibition (Fig. 4A). A similar mode of inhibition has been observed for INHs from potato [32,80–82], maize [57], tomato [73] and *Pteris deflexa* [83]. However, Sander et al. (1996) suggested that cell wall invertases could be protected against inhibition by sucrose, which would account for a competitive mode of inhibition [84].

As shown in Fig. 4, the slope (s), indicating that I binds to the free E, and the ordinate intercept, (i) showing that I binds to the enzyme–substrate complex (ES), increased with increasing SolyVIF concentrations (Fig. 4B and C). The secondary Lineweaver–Burk plots of sucrose hydrolysis (Fig. 4B and C) showing the slope (s) and the vertical axis intercept (i) against the inhibitor concentration can be described by a second-order polynome with respect to I, which corresponds to a parabolic equation with an excellent correlation coefficient (Equation (1)) [85]:

$$1/v_i = (a_0 + a_1[I] + a_2[I]^2) 1/[S] + b_0 + b_1[I] + b_2[I]^2 = s 1/[S] + i \quad (1)$$

where the coefficients (a_1, a_2, b_0, b_1, b_2) depending on the equilibrium constants correspond to the presence of EI, EI₂ and ESI, ESI₂ enzyme species in the reaction mixture. One and two SolyVIF molecules bind to both the free E and the ES complex, respectively. One model is proposed involving abortive complexes:



and consistent with the experimental data where the i and s equations (Eq. (2) and (3)) are:

$$i = \frac{1}{V} + \frac{1}{VL_{1i}}[I] + \frac{1}{VL_{1i}L_{2i}} + \frac{1}{VL_{1i}L_{2i}}[I]^2 \quad (2)$$

$$s = \frac{K_m}{V} + \frac{K_m}{\sqrt{K_{1i}}} [I] + \frac{K_m}{\sqrt{K_{1i}K_{2i}}} [I]^2 \quad (3)$$

Both i and s equations (Eq. (4) and (5)) are of a parabolic type:

$$i = d + e[I] + f[I]^2 \quad (4)$$

$$s = d' + e'[I] + f'[I]^2 \quad (5)$$

Kinetic parameters V, L_{1i} and L_{2i} were obtained from parameters d, e and f , which were calculated from the secondary plot (Fig. 4B). Using the V value thus obtained, kinetic parameters K_m, K_{1i} and K_{2i} were determined by the same way from parameters d', e' and f' calculated from plot of Fig. 4C.

Using the same calculations but with $[I] = 0$, the values of K_{1i}, K_{2i} and L_{1i}, L_{2i} were 122.6 nM, 5.05 nM and 110 nM and 5.07 nM, respectively (Table 2). The complexes EI and ESI are not formed when the initial velocity is measured, therefore no immediate inhibition could be observed until a concentration of 10 nM of SolyVIF is reached. The model is valid because the preincubation is of no effect and because binding of I to E or ES are slow reactions.

The values of the pseudo dissociation equilibrium constants K_{1i}, L_{1i} and K_{2i}, L_{2i} suggest that the EI and the ESI complexes are present in smaller amounts than EI₂ and ESI₂. It was previously reported that EI and ESI formation are slow processes [86,87]. In conclusion, the kinetic experiments in solution demonstrated that 2 molecules of inhibitor are able to bind to free E or the ES complex. The EI complex determined by SPR indicates an apparent stoichiometry 1:1 at equilibrium, probably because SPR cannot distinguish the additional binding site. The K_D value (for EI = 0.4 ± 0.2 nM) determined by SPR and K_{2i} (for EI₂ = 5.05 nM) and L_{2i} (for ESI₂ = 5.07 nM), determined by kinetic analysis in solution, demonstrate a very strong interaction between SolyVIF and TIV-1 in the nanomolar range with a ratio of 12 between the results obtained by the two methods. Such discrepancies between values obtained by different methods are quite common, and in our case may simply results from the fact that, while both techniques allow to investigate protein–protein interaction, kinetic experiments are performed in solution, while in SPR one of the partners is immobilized on a surface, which might prevent structural changes occurring upon complex formation. Moreover, the temperatures used in each assay were different, possibly accounting for the observed differences (see Material and methods section).

Recently, the crystal structure of the complex between AtcwINV1 and NtCIF [79], without substrate, has been reported. The

authors showed that in the enzyme/inhibitor complex a residue of the inhibitor (Lys98) inserts into the active site of AtcwINV1, where it interacts with the acid/base catalyst Glu203, thus blocking access for the substrate [79]. This mechanism corresponds to a competitive inhibition with formation of an EI complex. Thus, in this case, the absence of substrate during the crystallization process didn't

Table 2

The kinetic parameters, the inhibition constants and type of inhibition by SolyVIF for TIV-1 acting on sucrose. K_{i1} , K_{i2} , L_{i1} and L_{i2} are the EI, EI₂, ESI and ESI₂ related dissociation constants. The parameters were determined from secondary Lineweaver–Burk plots.

[Inhibitor] (nM)	k_{cat} (s ⁻¹)	K_m (mM)	k_{cat}/K_m (s ⁻¹ mM ⁻¹)	Inhibition %	K_{i1} (nM)	K_{i2} (nM)	L_{i1} (nM)	L_{i2} (nM)	Inhibition type
No SolyVIF	1328	12	110.7	0					
13.83	1159		96.6	12.7	122.6	5.05	110	5.07	Non-competitive
20.75	894		74.5	32.7					
27.6	652		54.3	51					

allow the formation of the ESI complex. Moreover, we can't rule out that the differences in the kinetic models arises from the fact that the kinetic model determined in the present work was achieved with vacuolar partners, which might bind together otherwise than enzymes and inhibitors from the cell wall compartment, as previously suggested by Sander et al. (1996) [84].

3.6. TIV-1 and SolyVIF interactions are pH dependent

Weil et al. had reported a strong pH-dependency for the inhibition of *N. tabacum* CWI by its inhibitor [34]. The structural basis for a similar pH dependency has recently been provided by the structural study of the AtcwINV1–NtCIF complex, coupled to isothermal titration calorimetry [79]. The AtcwINV1–NtCIF complex structure reveals a cluster of acidic residues that titrate in the relevant pH range. The close contact of these functional carboxylate groups implies that their protonation is required to allow interaction, and that a shift of pH towards more basic conditions would necessarily render the interactions unfavourable and disrupt the complex. To test whether the inhibition of TIV-1 by SolyVIF was dependent on pH, the inhibition of TIV-1 was measured at different pH values with constant amounts of SolyVIF (equivalent of 50% inhibition in optimal conditions). As shown in Fig. 5, inhibition occurs essentially in a tight pH range between 4.0 and 5.0, with a maximum at pH 4.5, which is the optimal pH of enzyme activity. It is noteworthy that most of the plant vacuoles are acidic and should the TIV-1/SolyVIF interaction be regulated *via* pH variations, this must occur in a pH range attainable within the vacuole.

3.7. TIV-1 and SolyVIF expression is tissue specific and regulated during plant development

The expression of TIV-1 and SolyVIF mRNAs was quantitatively analysed in different tissues by real-time PCR, and the results were

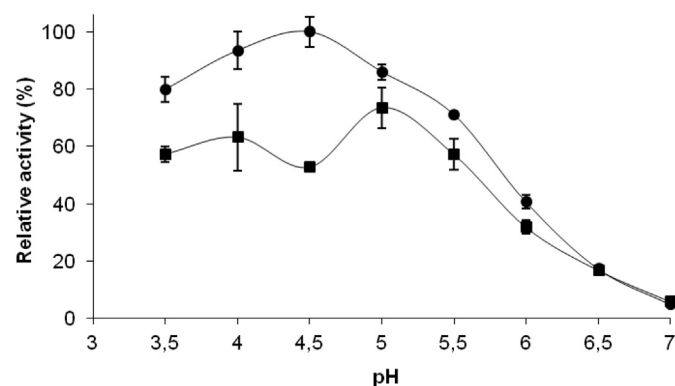


Fig. 5. Effect of pH on the relative activity of TIV-1 in the absence (circle) and presence (square) of SolyVIF (0.1 pmol to reach maximum of 50% inhibition in optimal conditions). Residual invertase activity was measured at pH 4.5 and 50 °C after an enzyme/inhibitor preincubation time of 10 min. Values depicted are the mean of duplicates based on at least three independent experiments.

normalized to the amount of *act-4* mRNA as reference gene (Fig. 6). The expression of both the vacuolar invertase and its inhibitor appeared to be tissue specific and developmentally regulated (Fig. 6). The highest level of expression of TIV-1 was detected in flowers in agreement with previous results showing a floral organ specific expression pattern with high level of expression in petals [88]. A higher level of expression of TIV-1 was also observed in red fruits as compared to green fruits. These findings are in good agreement with previous studies [88] and suggest a possible role of the vacuolar enzyme in source–sink sucrose metabolism during fruit ripening. The contribution of TIV-1 in tomato fruit growth and ripening was demonstrated in plants expressing a constitutive TIV-1 antisense gene. Transgenic TIV-1 antisense plants showed a dramatic alteration of soluble sugar composition, with elevated sucrose levels and changes in the concentration of osmotically active sugars, correlated with a reduced mature fruit size and indicating a role of TIV-1 in the regulation of turgor and cell enlargement during fruit maturation [89].

On the other hand, our transcript analysis shows a not significant expression of SolyVIF in flowers, as well as in both green and red fruits, indicating that its inhibition of TIV-1 activity is not relevant in flower tissue and during fruit ripening (Fig. 6). By contrast, CIF from *S. lycopersicum*, SolyCIF, was highly expressed in flowers and tomato green fruits [37], supporting the idea that CIFs and VIFs play different physiological roles.

Co-expression of SolyVIF and TIV-1 in sink tissues such as roots and stems, as well as in source leaves, points towards a role of SolyVIF in the post-transcriptional regulation of TIV-1 (Fig. 6). The co-expression was also observed in senescent leaves, suggesting that the posttranscriptional regulation of the vacuolar invertase by its inhibitory protein can play a role in controlling vacuolar sucrose hydrolysis during leaf senescence. The pivotal role of the post-transcriptional control of cell wall invertase activity by its inhibitor in leaf senescence has been demonstrated for tomato, where

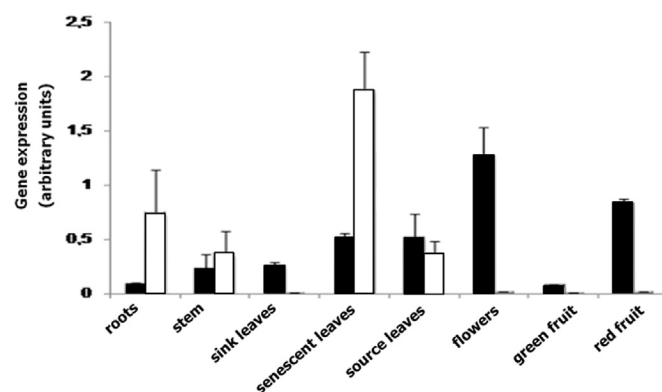


Fig. 6. Analysis of SolyVIF and TIV-1 expression in tomato tissues. The expression analysis of SolyVIF (white bars) and TIV-1 (black bars) in various tomato organs was determined using real-time qPCR. The relative level of gene expression was normalized with respect to *Act4* mRNA. Bars represent the average \pm SD ($n = 3$).

silencing of the *S. lycopersicum* inhibitor INVINH1 isoform in the plant increased the activity of cell wall invertase and significantly delayed abscisic acid induced leaf senescence [16].

Studies of tomato SolyVIF knock-out mutants or of plants overexpressing the inhibitor are under way to further explore the role(s) of this class of inhibitors during plant development.

Acknowledgements

We thank Dr. Ray Owens from the Department for Structural Biology at the University of Oxford for the pOPINF vector. Research performed in Marseille was funded by the Ministère de l'Enseignement Supérieur et de la Recherche Scientifique. Research performed in Italy was funded by the Institute Pasteur-Fondazione Cenci Bolognetti and by Ministero dell'Università e della Ricerca (PRIN 2010-11 2010T7247Z).

Appendix A. Supplementary data

Supplementary data related to this article can be found at <http://dx.doi.org/10.1016/j.biochi.2013.12.013>.

References

- [1] K. Koch, Sucrose metabolism: regulatory mechanisms and pivotal roles in sugar sensing and plant development, *Curr. Opin. Plant Biol.* 7 (2004) 235–246.
- [2] T. Roitsch, M.C. Gonzalez, Function and regulation of plant invertases: sweet sensations, *Trends Plant Sci.* 9 (2004) 606–613.
- [3] B.L. Cantarel, P.M. Coutinho, C. Rancurel, T. Bernard, V. Lombard, B. Henrissat, The carbohydrate-active enzymes database (CAZy): an expert resource for glycogenomics, *Nucleic Acids Res.* 37 (2009) D233–D238.
- [4] V. Fotopoulos, Plant invertases: structure, function and regulation of a diverse enzyme family, *J. Biol. Res.* 4 (2005) 127–137.
- [5] A. Sturm, Invertases. Primary structures, functions, and roles in plant development and sucrose partitioning, *Plant Physiol.* 121 (1999) 1–8.
- [6] M.A. Hayes, C. Davies, I.B. Dry, Isolation, functional characterization, and expression analysis of grapevine (*Vitis vinifera* L.) hexose transporters: differential role in sink and source tissues, *J. Exp. Bot.* 58 (2007) 1985–1997.
- [7] E. Wang, J. Wang, X. Zhu, W. Hao, L. Wang, Q. Li, L. Zhang, W. He, B. Lu, H. Lin, H. Ma, G. Zhang, Z. He, Control of rice grain-filling and yield by a gene with a potential signature of domestication, *Nat. Genet.* 40 (2008) 1370–1374.
- [8] M.I. Zanor, S. Osorio, A. Nunes-Nesi, F. Carrari, M. Lohse, B. Usadel, C. Kuhn, W. Bleiss, P. Giavalisco, L. Willmitzer, R. Sulpice, Y.H. Zhou, A.R. Fernie, RNA interference of LIN5 in tomato confirms its role in controlling Brix content, uncovers the influence of sugars on the levels of fruit hormones, and demonstrates the importance of sucrose cleavage for normal fruit development and fertility, *Plant Physiol.* 150 (2009) 1204–1218.
- [9] J. Essmann, I. Schmitz-Thom, H. Schon, S. Sonnewald, E. Weis, J. Scharte, RNA interference-mediated repression of cell wall invertase impairs defense in source leaves of tobacco, *Plant Physiol.* 147 (2008) 1288–1299.
- [10] M.A. Hayes, A. Feechan, I.B. Dry, Involvement of abscisic acid in the coordinated regulation of a stress-inducible hexose transporter (VvHT5) and a cell wall invertase in grapevine in response to biotrophic fungal infection, *Plant Physiol.* 153 (2010) 211–221.
- [11] N. Kocal, U. Sonnewald, S. Sonnewald, Cell wall-bound invertase limits sucrose export and is involved in symptom development and inhibition of photosynthesis during compatible interaction between tomato and *Xanthomonas campestris* pv *vesicatoria*, *Plant Physiol.* 148 (2008) 1523–1536.
- [12] H. Tian, Q. Kong, Y. Feng, X. Yu, Cloning and characterization of a soluble acid invertase-encoding gene from muskmelon, *Mol. Biol. Rep.* 36 (2009) 611–617.
- [13] X. Yu, X. Wang, W. Zhang, T. Qian, G. Tang, Y. Guo, C. Zheng, Antisense suppression of an acid invertase gene (MAI1) in muskmelon alters plant growth and fruit development, *J. Exp. Bot.* 59 (2008) 2969–2977.
- [14] C. Davies, S.P. Robinson, Sugar accumulation in grape berries. Cloning of two putative vacuolar invertase cDNAs and their expression in grapevine tissues, *Plant Physiol.* 111 (1996) 275–283.
- [15] S. Greiner, T. Rausch, U. Sonnewald, K. Herbers, Ectopic expression of a tobacco invertase inhibitor homolog prevents cold-induced sweetening of potato tubers, *Nat. Biotechnol.* 17 (1999) 708–711.
- [16] Y. Jin, D.A. Ni, Y.L. Ruan, Posttranslational elevation of cell wall invertase activity by silencing its inhibitor in tomato delays leaf senescence and increases seed weight and fruit hexose level, *Plant Cell* 21 (2009) 2072–2089.
- [17] R. Pressey, R. Shaw, Effect of temperature on invertase, invertase inhibitor, and sugars in potato tubers, *Plant Physiol.* 41 (1966) 1657–1661.
- [18] P.K. Koonjul, J.S. Minhas, C. Nunes, I.S. Sheoran, H.S. Saini, Selective transcriptional down-regulation of anther invertases precedes the failure of pollen development in water-stressed wheat, *J. Exp. Bot.* 56 (2005) 179–190.
- [19] Y. Zeng, Y. Wu, W.T. Avigne, K. Koch, Rapid repression of maize invertases by low oxygen. Invertase/sucrose synthase balance, sugar signaling potential, and seedling survival, *Plant Physiol.* 121 (1999) 599–608.
- [20] L.L. Wu, I. Song, N. Karupiah, P.B. Kaufman, Kinetic induction of oat shoot pulvinus invertase mRNA by gravistimulation and partial cDNA cloning by the polymerase chain reaction, *Plant Mol. Biol.* 21 (1993) 1175–1179.
- [21] W.A. Vargas, G.L. Salerno, The Cinderella story of sucrose hydrolysis: alkaline/neutral invertases, from cyanobacteria to unforeseen roles in plant cytosol and organelles, *Plant Sci.* 178 (2010) 1–8.
- [22] L. Xiang, Y. Li, F. Rolland, W. Van den Ende, Neutral invertase, hexokinase and mitochondrial ROS homeostasis. Emerging links between sugar metabolism, sugar signaling and ascorbate synthesis, *Plant Signal. Behav.* 6 (2011) 1567–1573.
- [23] L.F. Huang, P. Cocco, J. Davis, K. Koch, Regulation of invertase: a 'suite' of transcriptional and post-transcriptional mechanisms, *Funct. Plant Biol.* 34 (2007) 499–507.
- [24] T. Roitsch, M.E. Balibrea, M. Hofmann, R. Proels, A.K. Sinha, Extracellular invertase: key metabolic enzyme and PR protein, *J. Exp. Bot.* 54 (2003) 513–524.
- [25] G. Kern, N. Schulke, F.X. Schmid, R. Jaenicke, Stability, quaternary structure, and folding of internal, external, and core-glycosylated invertase from yeast, *Protein Sci.* 1 (1992) 120–131.
- [26] G. Kern, D. Kern, R. Jaenicke, R. Seckler, Kinetics of folding and association of differently glycosylated variants of invertase from *Saccharomyces cerevisiae*, *Protein Sci.* 2 (1993) 1862–1868.
- [27] M. Tammi, L. Ballou, A. Taylor, C.E. Ballou, Effect of glycosylation on yeast invertase oligomer stability, *J. Biol. Chem.* 262 (1987) 4395–4401.
- [28] U. Andjelkovic, S. Theissen, H.A. Scheidt, M. Petkovic, D. Huster, Z. Vujcic, The thermal stability of the external invertase isoforms from *Saccharomyces cerevisiae* correlates with the surface charge density, *Biochimie* 94 (2012) 510–515.
- [29] L. Faye, M.J. Chrispeels, Apparent inhibition of beta-fructosidase secretion by tunicamycin may be explained by breakdown of the unglycosylated protein during secretion, *Plant Physiol.* 89 (1989) 845–851.
- [30] S. Pagny, L.A. Denmat-Ouisse, V. Gomord, L. Faye, Fusion with HDEL protects cell wall invertase from early degradation when N-glycosylation is inhibited, *Plant Cell Physiol.* 44 (2003) 173–182.
- [31] A. Sturm, Heterogeneity of the complex N-linked oligosaccharides at specific glycosylation sites of two secreted carrot glycoproteins, *Eur. J. Biochem.* 199 (1991) 169–179.
- [32] S. Schwimmer, R.U. Makower, E.S. Rorem, Invertase & invertase inhibitor in potato, *Plant Physiol.* 36 (1961) 313–316.
- [33] R. Pressey, Separation and properties of potato invertase and invertase inhibitor, *Arch. Biochem. Biophys.* 113 (1966) 667–674.
- [34] M. Weil, S. Krausgrill, A. Schuster, T. Rausch, A 17-kDa *Nicotiana tabacum* cell-wall peptide acts as an in-vitro inhibitor of the cell-wall isoform of acid invertase, *Planta* 193 (1994) 438–445.
- [35] M. Link, T. Rausch, S. Greiner, In *Arabidopsis thaliana*, the invertase inhibitors AtC/VIF1 and 2 exhibit distinct target enzyme specificities and expression profiles, *FEBS Lett.* 573 (2004) 105–109.
- [36] I. Privat, S. Foucrier, A. Prins, T. Epalle, M. Eychemme, L. Kandalaf, V. Caillet, C. Lin, S. Tanksley, C. Foyer, J. McCarthy, Differential regulation of grain sucrose accumulation and metabolism in *Coffea arabica* (Arabica) and *Coffea canephora* (Robusta) revealed through gene expression and enzyme activity analysis, *New Phytol.* 178 (2008) 781–797.
- [37] I.B. Reça, A. Brutus, R. D'Avino, C. Villard, D. Bellincampi, T. Giardina, Molecular cloning, expression and characterization of a novel apoplasmic invertase inhibitor from tomato (*Solanum lycopersicum*) and its use to purify a vacuolar invertase, *Biochimie* 90 (2008) 1611–1623.
- [38] M. Hothorn, S. Wolf, P. Aloy, S. Greiner, K. Scheffzek, Structural insights into the target specificity of plant invertase and pectin methylesterase inhibitory proteins, *Plant Cell* 16 (2004) 3437–3447.
- [39] D.A. Brummell, R.K. Chen, J.C. Harris, H. Zhang, C. Hamiaux, A.V. Kralicek, M.J. McKenzie, Induction of vacuolar invertase inhibitor mRNA in potato tubers contributes to cold-induced sweetening resistance and includes spliced hybrid mRNA variants, *J. Exp. Bot.* 62 (2011) 3519–3534.
- [40] X. Liu, B. Song, H. Zhang, X.Q. Li, C. Xie, J. Liu, Cloning and molecular characterization of putative invertase inhibitor genes and their possible contributions to cold-induced sweetening of potato tubers, *Mol. Genet. Gen.* 284 (2010) 147–159.
- [41] X. Liu, Y. Lin, J. Liu, B. Song, Y. Ou, H. Zhang, M. Li, C. Xie, StInVlnh2 as an inhibitor of StvacINV1 regulates the cold-induced sweetening of potato tubers by specifically capping vacuolar invertase activity, *Plant Biotechnol. J.* 11 (2013) 640–647.
- [42] K.B. Bonfig, A. Gabler, U.K. Simon, N. Luschin-Ebengreuth, M. Hatz, S. Berger, N. Muhammad, J. Zeier, A.K. Sinha, T. Roitsch, Post-translational derepression of invertase activity in source leaves via down-regulation of invertase inhibitor expression is part of the plant defense response, *Mol. Plant* 3 (2011) 1037–1048.
- [43] Y. Lin, J. Liu, X. Liu, Y. Ou, M. Li, H. Zhang, B. Song, C. Xie, Interaction proteins of invertase and invertase inhibitor in cold-stored potato tubers suggested a protein complex underlying post-translational regulation of invertase, *Plant Physiol. Biochem.* 73 (2013) 237–244.
- [44] S. Westphal, D. Kolarich, K. Foetisch, I. Lauer, F. Altmann, A. Conti, J.F. Crespo, J. Rodriguez, E. Enrique, S. Vieths, S. Scheurer, Molecular characterization and

- allergenic activity of Lyc e 2 (β -fructofuranosidase), a glycosylated allergen of tomato, *Eur. J. Biochem.* 270 (2003) 1327–1337.
- [45] M. Lafond, A. Tauzin, V. Desseaux, E. Bonnin, E.H. Ajandouz, T. Giardina, GH10 xylanase D from *Penicillium funiculosum*: biochemical studies and xylooligosaccharide production, *Microb. Cell Fact.* 10 (2011) 20.
- [46] A. Brutus, I.B. Reça, S. Herga, B. Mattei, A. Puigserver, J.C. Chaix, N. Juge, D. Bellincampi, T. Giardina, A family 11 xylanase from the pathogen *Botrytis cinerea* is inhibited by plant endoxylanase inhibitors XIP-I and TAXI-I, *Biochem. Biophys. Res. Commun.* 337 (2005) 160–166.
- [47] W.R. McClachlan, M.T. Garcia-Conesa, G. Williamson, M. Roza, P. Ravestain, J. Maat, A novel class of protein from wheat which inhibits xylanases, *Biochem. J.* 338 (1999) 441–446.
- [48] S. Fazekas de St Groth, R.G. Webster, A. Datyner, Two new staining procedures for quantitative estimation of proteins on electrophoretic strips, *Biochem. Biophys. Acta* 71 (1963) 377–391.
- [49] M.M. Bradford, A rapid and sensitive method for the quantification of microgram quantities of protein utilizing the principle of protein-dye binding, *Anal. Biochem.* 72 (1976) 248–254.
- [50] M.W. Pfaffl, A new mathematical model for relative quantification in real-time RT-PCR, *Nucleic Acids Res.* 29 (2001) e45.
- [51] J.D. Thompson, D.G. Higgins, T.J. Gibson, CLUSTAL W: improving the sensitivity of progressive multiple sequence alignment through sequence weighting, position specific gap penalties and weight matrix choice, *Nucleic Acids Res.* 22 (1994) 4673–4680.
- [52] P. Gouet, X. Robert, E. Courcelle, ESPript/ENDscript: extracting and rendering sequence and 3D information from atomic structures of proteins, *Nucleic Acids Res.* 31 (2003) 3320–3323.
- [53] W.L. Delano, The PyMOL molecular graphics system, Delano Scientific, San Carlos, CA, USA, [http://www.pymol.org].
- [54] Z. Tymowska-Lalanne, M. Kreis, The plant invertases: physiology, biochemistry and molecular biology, *Adv. Bot. Res.* 28 (1998) 71–117.
- [55] L. Xiang, W. Van den Ende, Trafficking of plant vacuolar invertases: from a membrane-anchored to a soluble status. Understanding sorting information in their complex N-terminal motifs, *Plant Cell Physiol.* 54 (2013) 1263–1277.
- [56] X. Tang, H.P. Ruffner, J.D. Scholes, S.A. Rolfe, Purification and characterisation of soluble invertases from leaves of *Arabidopsis thaliana*, *Planta* 198 (1996) 17–23.
- [57] T.A. Jaynes, O.E. Nelson, An invertase inactivator in maize endosperm and factors affecting inactivation, *Plant Physiol.* 47 (1971) 629–634.
- [58] V.J. Nagaraj, V. Galati, M. Luscher, T. Boller, A. Wiemken, Cloning and functional characterization of a cDNA encoding barley soluble acid invertase (HvINV1), *Plant Sci.* 168 (2005) 249–258.
- [59] W.C. Huang, A.Y. Wang, L.T. Wang, H.Y. Sung, Expression and characterization of sweet potato invertase in *Pichia pastoris*, *J. Agric. Food Chem.* 51 (2003) 1494–1499.
- [60] L.T. Wang, A.Y. Wang, C.W. Hsieh, C.Y. Chen, H.Y. Sung, Vacuolar invertases in sweet potato: molecular cloning, characterization, and analysis of gene expression, *J. Agric. Food Chem.* 53 (2005) 3672–3678.
- [61] X. Ji, W. Van den Ende, L. Schroeven, S. Clerens, K. Geuten, S. Cheng, J. Bennett, The rice genome encodes two vacuolar invertases with fructan exohydrolase activity but lacks the related fructan biosynthesis genes of the Pooideae, *New Phytol.* 173 (2007) 50–62.
- [62] L. Schroeven, W. Lammens, A. Van Laere, W. Van den Ende, Transforming wheat vacuolar invertase into a high affinity sucrose:sucrose 1-fructosyltransferase, *New Phytol.* 180 (2008) 822–831.
- [63] V. Barba Cedillo, F.J. Plou, M. Jesús Martínez, Recombinant sterol esterase from *Ophiostoma piceae*: an improved biocatalyst expressed in *Pichia pastoris*, *Microb. Cell Fact.* 11 (2012) 73.
- [64] W. Lammens, K. Le Roy, S. Yuan, R. Vergauwen, A. Rabijn, A. Van Laere, S.V. Strelkov, W. Van den Ende, Crystal structure of 6-SST/6-SFT from *Pachysandra terminalis*, a plant fructan biosynthesizing enzyme in complex with its acceptor substrate 6-kestose, *Plant J.* 70 (2012) 205–219.
- [65] M. Verhaest, W. Lammens, K. Le Roy, B. De Coninck, C.J. De Ranter, A. Van Laere, W. Van den Ende, A. Rabijns, X-ray diffraction structure of a cell-wall invertase from *Arabidopsis thaliana*, *Acta Crystallogr. D Biol. Crystallogr.* 62 (2006) 1555–1563.
- [66] M. Verhaest, W. Van den Ende, K. Le Roy, C.J. De Ranter, A. Van Laere, A. Rabijns, X-ray diffraction structure of a plant glycosyl hydrolase family 32 protein: fructan 1-exohydrolase IIa of *Cichorium intybus*, *Plant J.* 41 (2005) 400–411.
- [67] R.A. Nagem, A.L. Rojas, A.M. Golubev, O.S. Korneeva, E.V. Eneyskaya, A.A. Kulminskaya, K.N. Neustroev, I. Polikarpov, Crystal structure of exoinulinase from *Aspergillus awamori*: the enzyme fold and structural determinants of substrate recognition, *J. Mol. Biol.* 19 (2004) 471–480.
- [68] J.L. Cereghino, J.M. Cregg, Heterologous protein expression in the methylotrophic yeast *Pichia pastoris*, *FEMS Microbiol. Rev.* 24 (2000) 45–66.
- [69] R.K. Bretthauer, F.J. Castellino, Glycosylation of *Pichia pastoris*-derived protein, *Biotechnol. Appl. Biochem.* 30 (1999) 193–200.
- [70] M.L. Wang, L.S. Lee, A. Nepomich, J.D. Yang, C. Conover, M. Whitlow, D. Filpula, Single-chain Fv with manifold N-glycans as bifunctional scaffolds for immunomolecules, *Protein Eng.* 11 (1998) 1277–1283.
- [71] K. Le Roy, M. Verhaest, A. Rabijns, S. Clerens, A. Van Laere, W. Van den Ende, N-Glycosylation affects substrate specificity of chicory fructan 1-exohydrolase: evidence for the presence of an inulin binding cleft, *New Phytol.* 176 (2007) 317–324.
- [72] G.E. Bracho, J.R. Whitaker, Purification and partial characterization of potato (*Solanum tuberosum*) invertase and its endogenous proteinaceous inhibitor, *Plant Physiol.* 92 (1990) 386–394.
- [73] R. Pressey, Invertase inhibitor in tomato fruit, *Phytochemistry* 36 (1994) 543–546.
- [74] Y.L. Wang, C.Y. Wu, C.T. Chang, H.Y. Sung, Invertase inhibitors from sweet potato (*Ipomoea batatas*): purification and biochemical characterization, *J. Agric. Food Chem.* 51 (2003) 4804–4809.
- [75] N.J. Bate, X. Niu, Y. Wang, K.S. Reimann, T.G. Helentjaris, An invertase inhibitor from maize localizes to the embryo surrounding region during early kernel development, *Plant Physiol.* 134 (2004) 246–254.
- [76] S. Greiner, S. Krausgrill, T. Rausch, Cloning of a tobacco apoplasmic invertase inhibitor – proof of function of the recombinant protein and expression analysis during plant development, *Plant Physiol.* 116 (1998) 733–742.
- [77] M. Hothorn, I. D'Angelo, J.A. Marquez, S. Greiner, K. Scheffzek, The invertase inhibitor Nt-CIF from tobacco: a highly thermostable four-helix bundle with an unusual N-terminal extension, *J. Mol. Biol.* 335 (2004) 987–995.
- [78] A. Di Matteo, A. Giovane, A. Raiola, L. Camardella, D. Bonivento, G. De Lorenzo, F. Cervone, D. Bellincampi, D. Tsernoglou, Structural basis for the interaction between pectin methylesterase and a specific inhibitor protein, *Plant Cell* 17 (2005) 849–858.
- [79] M. Hothorn, W. Van den Ende, W. Lammens, V. Rybin, K. Scheffzek, Structural insights into the pH-controlled targeting of plant cell-wall invertase by a specific inhibitor protein, *Proc. Natl. Acad. Sci. U. S. A.* 107 (2010) 17427–17432.
- [80] R. Pressey, Invertase inhibitor from potatoes: purification, characterization, and reactivity with plant invertases, *Plant Physiol.* 42 (1967) 1780–1786.
- [81] E.E. Ewing, M.H. McAadoo, An examination of methods used to assay potato tuber invertase and its naturally occurring inhibitor, *Plant Physiol.* 48 (1971) 366–370.
- [82] G.E. Bracho, J.R. Whitaker, Characteristics of the inhibition of potato (*Solanum tuberosum*) invertase by an endogenous proteinaceous inhibitor in potatoes, *Plant Physiol.* 92 (1990) 381–385.
- [83] J.E. Sayago, M.A. Vattuone, A.R. Sampietro, M.I. Isla, An invertase inhibitory protein from *Pteris deflexa* link fronds, *J. Enzyme Inhib.* 16 (2001) 517–525.
- [84] A. Sander, S. Krausgrill, S. Greiner, M. Weil, T. Rausch, Sucrose protects cellwall invertase but not vacuolar invertase against proteinaceous inhibitors, *FEBS Lett.* 385 (1996) 171–175.
- [85] M. Alkazaz, V. Desseaux, G. Marchis-Mouren, F. Payan, E. Forest, M. Santimone, The mechanism of porcine pancreatic α -amylase. Kinetic evidence for two additional carbohydrate-binding sites, *Eur. J. Biochem.* 241 (1996) 787–796.
- [86] V. Le Berre-Anton, C. Bompard-Gilles, F. Payan, P. Rouge, Characterization and functional properties of the α -amylase inhibitor (α -AI) from kidney bean (*Phaseolus vulgaris*) seeds, *Biochim. Biophys. Acta* 1343 (1997) 31–40.
- [87] M. Santimone, R. Koukiekolo, Y. Moreau, V. Le Berre, P. Rouge, G. Marchis-Mouren, V. Desseaux, Porcine pancreatic α -amylase inhibition by the kidney bean (*Phaseolus vulgaris*) inhibitor (α -AI1) and structural changes in the α -amylase inhibitor complex, *Biochim. Biophys. Acta* 1646 (2004) 181–190.
- [88] D.E. Godt, T. Roitsch, Regulation and tissue-specific distribution of mRNAs for three extracellular invertase isoenzymes of tomato suggests an important function in establishing and maintaining sink metabolism, *Plant Physiol.* 115 (1997) 273–282.
- [89] E.M. Klann, B. Hall, A.B. Bennett, Antisense acid invertase (TIV1) gene alters soluble sugar composition and size in transgenic tomato fruit, *Plant Physiol.* 112 (1996) 1321–1330.